A NONDESTRUCTIVE EVALUATION TECHNIQUE FOR FIBER REINFORCED POLYMER (FRP) COMPOSITES USING ACOUSTIC GUIDED WAVES (AGW)

J.C. Trovillion*
US Army Engineer Research and Development Center
Construction Engineering Research Laboratory
Champaign, IL 61822-1076

V.F. Godínez-Azcuaga, R.D. Finlayson
Physical Acoustics Corporation
Princeton Junction, NJ 08550

ABSTRACT

In this paper, the predictions of the theoretical model and results obtained in the inspection of FRP wraps on concrete samples with seeded defects are presented. Additionally, the successful use of this NDE technique in the detection and imaging of delaminations, debonds, cracks and steel reinforcement in FRP-Concrete structures are discussed. These results are presented in the form of displayed RF waveforms and color-coded C-scan images. Finally, a description of a prototype inspection system for FRP-retrofitted concrete structures developed during the Phase II of the project is presented.

1. INTRODUCTION

To increase, or maintain, the strength of buildings, bridges, and concrete water and sewer pipes for carrying capacity, additional tension-carrying materials, such as Fiber Reinforced Polymer (FRP) composites, are being used. Efficient use of FRP composites to increase the strength of concrete structures depends on proper bonding between the FRP and the concrete structure. It is therefore very important that any defects present at the interface, within the composite, or cracks open to the concrete surface are detected in order to maintain the structural integrity of the reinforced concrete structure.

Since composites are complex and possess anisotropic material properties, they are very difficult to inspect using conventional nondestructive evaluation methods. Through a Small Business Innovative Research (SBIR) Project titled *"Field Portable Infrastructure Fiber-Reinforced Polymer Composite Inspection & Evaluation System using Ultrasound Technologies"* with the US Army Corps of Engineers, Engineering Research and Development Center – Construction Engineering Research Laboratory (ERDC-CERL), Physical Acoustics Corporation (PAC) developed an NDE technique for inspecting FRP retrofitted concrete and masonry structures. The technical aspects of the technique were studied during Phase I and Phase I Option of the project. During Phase II, PAC designed and constructed a field-portable inspection system for the nondestructive inspection of FRP retrofitted concrete structures. At the completion of Phase II in January 2004, the FRP-Concrete Inspection System (FRPCIS) was delivered to ERDC-CERL.

The FRPCIS was developed on a hand-held computer platform and uses a newly developed probe equipped with acoustic rolling sensors and mechanical encoders for position tracking. FRPCIS is capable of displaying RF waveforms and processing the data to produce C-scan images of the inspected structures. FRPCIS is used for inspecting seismic retrofits in Army facilities, however, the system could be used on other Army applications of thin layered FRP composites. These include the composite skins in planes and helicopters, blast protection fabric systems, rotorcraft blades, and ballistic protective inserts (BPI) in personnel armor (Godinez et al, 2002).

2. PHASE I RESEARCH

In December 2000 ERDC-CERL awarded PAC a Phase I, SBIR project entitled "Field Portable Infrastructure Fiber-Reinforced Polymer Composite Inspection & Evaluation System Using Ultrasound Technologies". In this Phase I study, the goal was to demonstrate the feasibility of using Guided Wave Acousto-Ultrasonics (AU) for the inspection of civil engineering structures retrofitted with FRP. In order to achieve this goal, PAC performed theoretical simulations to analyze the characteristics of wave propagation on FRP retrofitted concrete samples with and without defects. Based on the results of the wave propagation simulation, experiments were designed and performed on FRP-concrete samples fabricated at PAC. The data collected from the experimental results and the theoretical predictions were in very good agreement. Also, wave propagation data were collected on real FRP retrofitted concrete samples provided by ERDC-CERL. C-scan images of sections of the samples were generated.

Report Documentation Page

Form Approved
OMB No. 0704-0188

1. REPORT DATE **00 DEC 2004**	2. REPORT TYPE **N/A**	3. DATES COVERED **-**

4. TITLE AND SUBTITLE **A Nondestructive Evaluation Technique For Fiber Reinforced Polymer (Frp) Composites Using Acoustic Guided Waves (Agw)**	5a. CONTRACT NUMBER 5b. GRANT NUMBER 5c. PROGRAM ELEMENT NUMBER
6. AUTHOR(S)	5d. PROJECT NUMBER 5e. TASK NUMBER 5f. WORK UNIT NUMBER
7. PERFORMING ORGANIZATION NAME(S) AND ADDRESS(ES) **US Army Engineer Research and Development Center Construction Engineering Research Laboratory Champaign, IL 61822-1076 Physical Acoustics Corporation Princeton Junction, NJ 08550**	8. PERFORMING ORGANIZATION REPORT NUMBER
9. SPONSORING/MONITORING AGENCY NAME(S) AND ADDRESS(ES)	10. SPONSOR/MONITOR’S ACRONYM(S) 11. SPONSOR/MONITOR’S REPORT NUMBER(S)

12. DISTRIBUTION/AVAILABILITY STATEMENT
Approved for public release, distribution unlimited

13. SUPPLEMENTARY NOTES
See also ADM001736, Proceedings for the Army Science Conference (24th) Held on 29 November - 2 December 2005 in Orlando, Florida. , The original document contains color images.

14. ABSTRACT

15. SUBJECT TERMS

16. SECURITY CLASSIFICATION OF:			17. LIMITATION OF ABSTRACT	18. NUMBER OF PAGES	19a. NAME OF RESPONSIBLE PERSON
a. REPORT	b. ABSTRACT	c. THIS PAGE			
unclassified	**unclassified**	**unclassified**	**UU**	**8**	

Standard Form 298 (Rev. 8-98)
Prescribed by ANSI Std Z39-18

2.1 Wave Propagation Model

A theoretical model was used to simulate the propagation of acoustic waves in a concrete structure reinforced with a +/- 45 degree graphite/epoxy "wrap" with and without debonds between the concrete and the composite "wrap". This model simulates the propagation of an acoustic plane wave in a layered structure, by using the Thomson-Haskell transfer matrix for multilayered media in order to obtain the internal distribution of the energy vector within the FRP/concrete structure (Ji et al, 1996). The theoretical model also provides ultrasonic response in the forms reflection and transmission coefficient plots as a function of incidence angle, and frequency of the ultrasonic wave.

Figure 1 shows the experimental setup on which the model is based. The system is a +/- 45 degree graphite/epoxy 3mm thick layer laid on top of a 100mm concrete substrate, with a debond located between the layer and the substrate.

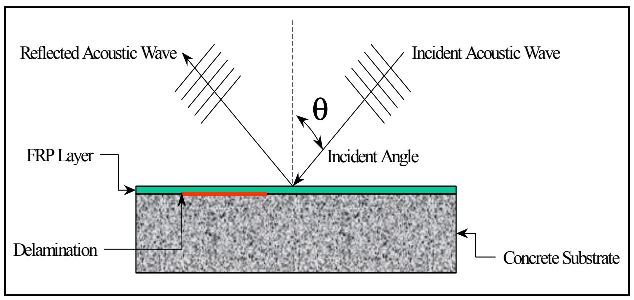

Figure 1. Setup used for the theoretical simulation of wave propagation on FRP-concrete structures

Figure 2 shows a plot of the reflection coefficient for acoustic waves propagating on the FRP-concrete layered structure without debonds. In this plot, the areas in bright red indicate a very high reflection coefficient, with a maximum value of 1, and the dark blue areas indicate very low reflection. Acoustic waves with a combination of frequency-incidence angle that lie on the bright red areas will be reflected almost completely whereas acoustic waves with a combination of frequency-incidence angle that lie on the blue spots will not present a high reflection. This type of plot is very useful when analyzing the changes in the reflection coefficient produced by the presence of a delamination in the structure. Figure 3 shows a similar plot but this time a delamination was introduced between the layer of FRP and the concrete substrate.

2.2 Theoretical Predictions

The model discussed in section 2.1 was used to calculate the reflection coefficients for the FRP/concrete structure with and without debonds between the FRP and

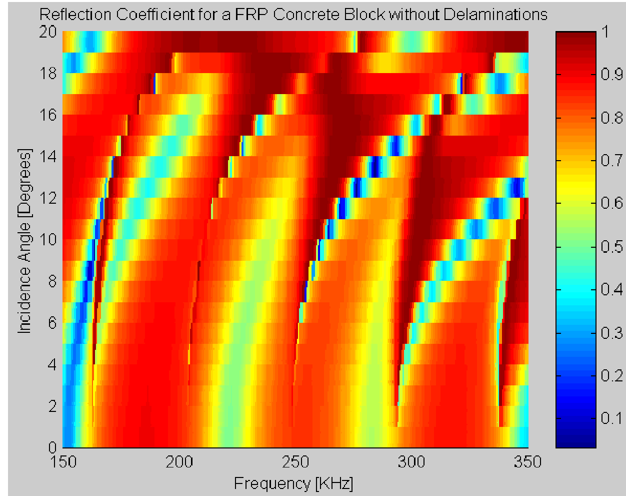

Figure 2. Reflection coefficient of an FRP-concrete layered structure without debonds.

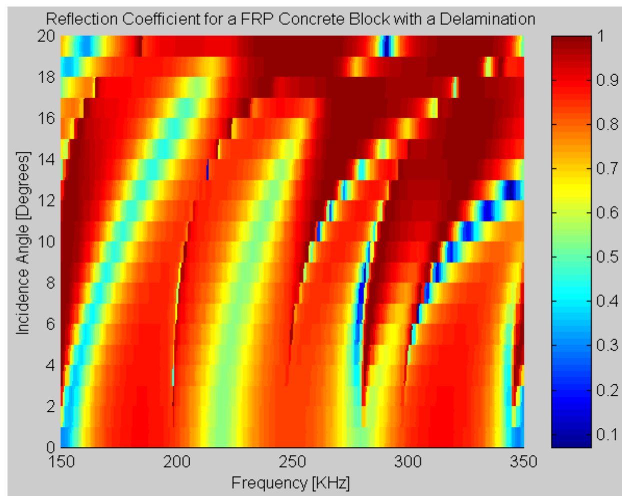

Figure 3. Reflection coefficient of an FRP-concrete layered structure with a debond between the FRP and the concrete.

the concrete substrate for an incidence angle of 0 degrees. This angle of incidence was selected because the sensors used in the rolling probe send an acoustic beam normal to the surface of the FRP. Figure 4 shows the results of these calculations.

The reflection coefficient calculated for the FRP-concrete structure without debonds is represented by the green plot. This plot shows a minimum at approximately 340 kHz. The reflection coefficient for the structure with debonds, represented by the red plot, shows a similar behavior but the position of the minimum has shifted to approximately 260 kHz.

The results shown in Figure 4 indicate that there are two frequencies, at which the difference between reflection coefficients of the bonded and debonded FRP-

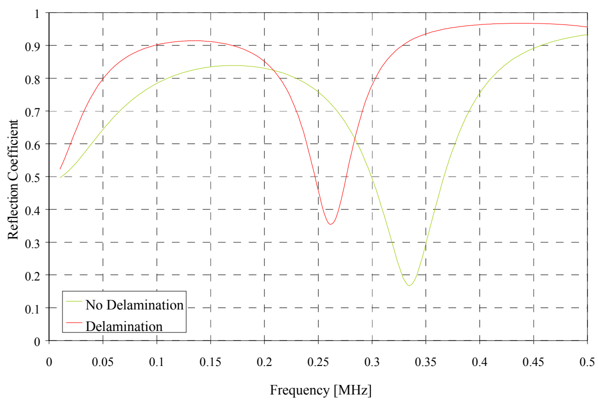

Figure 4. Theoretical prediction of reflection coefficient from an FRP/Concrete structure with a debond (red) and without a debond (green) as function of frequency for normal incidence.

concrete sample is large enough to allow the detection of the debond itself. These frequencies correspond to the minima of the reflection coefficients at 260 and 340 kHz.

The difference between the reflection coefficients shown in Figure 4 is called the Contrast Index (CI), and it is an indication of how much the amplitude of the reflected acoustic signal will change from an area of the FRP/Concrete structure without debonds to an area where debonds are present between the FRP and the concrete (Godinez et al, 2001). This parameter, as with the reflection coefficient, is as function of frequency. Figure 5 shows the CI calculated using the reflection coefficients of Figure 4.

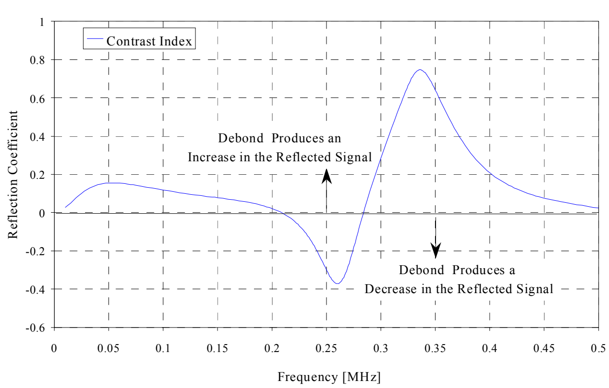

Figure 5. Contrast Index as a function of frequency for an FRP/Concrete structure with debonds between the composite and the concrete.

The Figure 5 plot indicates that if the CI value is lower than 0, the debond produces a decrease in the amplitude of the reflected signal. This is the case for the 260 kHz frequency component in Figure 5. On the contrary if the CI value is greater than 0, the presence of a debond will increase the amplitude of the reflected acoustic signal, as in the case of the 340 KHz frequency component. In both cases, the larger the absolute value of the CI, the better the contrast that a debond will present on a C-scan image against the background of an undamaged area.

The CI plot resulting from the simulation is useful in choosing the best frequency range to perform the inspection, according to the type of structure and the position defect within it. In the case of the FRP/Concrete structure either, 260 or 340 kHz are inspection frequencies which increase the probability of detecting debonds.

2.3 Experimental Work

The experimental work performed to demonstrate the feasibility of using the AU technique in the inspection of FRP/concrete structures was carried out on samples of FRP/concrete with seeded defects. These defects include cracks on the concrete, debonds between the FRP and the concrete and delaminations in the FRP. The debonds and delaminations were generated by inserting teflon wafers between the concrete and the FRP, for the case of the debonds, and between two layers of the FRP "wrap" in the case of delaminations. Cracks were introduced in the concrete by "three point bending" the concrete samples before applying the FRP "wrap".

The sensors used in the work were PAC's differential rolling sensor (RSWD). The rolling sensor rubber tire acts as a dry couplant between the sensor and the surface of the FRP-concrete sample and maintains a constant distance from the FRP-concrete sample therefore reducing the reflected amplitude changes caused by the contact variation between the sensor and the structure. Figure 6 shows a picture of two RSWD mounted on a scanning bridge during inspection of an FRP-concrete sample. Figure 7 shows a detail of the rolling sensors in contact with the FRP/Concrete sample.

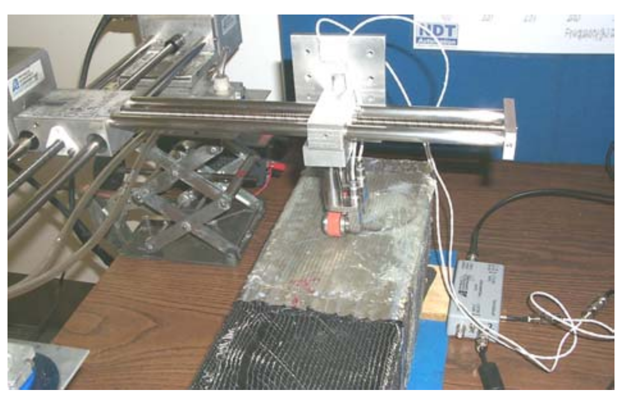

Figure 6. Inspection of a FRP-concrete sample using rolling sensors mounted on a scanning bridge.

A series of C-scan images were generated on the FRP/Concrete samples using RSWD rolling sensors as

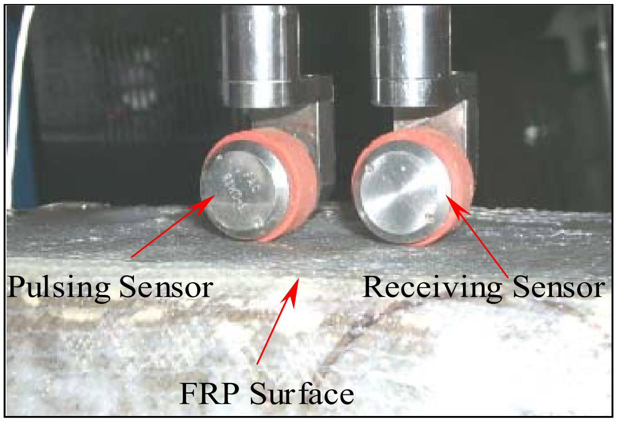

Figure 7. Detail of the rolling sensors during Inspection of an FRP/concrete sample.

pulser and receiver. The sensor separation was 1.5 inches from center to center. A 10 cycle-260 kHz square wave tone burst with constant amplitude signal was used to excite the pulsing sensor.

Before scanning the samples with seeded defects, RF signals were acquired on top of a well bonded and a debonded area of one of the samples. As predicted by the theory, the acoustic signal recorded on top of the debonded area shows a reduction in amplitude with respect to the signal recorded on the well-bonded area. The RF signals corresponding to the bonded and debonded areas are shown in Figures 8(a) and 8(b) respectively.

Figure 9 shows a C-scan of an FRP/Concrete sample that contains a debond between the FRP and the concrete. This debond is clearly visible in the image as a red area over a green background. The color palette of the C-scan image was set to show areas of reflected signals with large amplitudes in dark green color, and signals with small reflected amplitudes in red. Therefore, the red spot in the image of Figure 9, which corresponds to the presence of a debond, indicates a drop in the amplitude of the reflected signal, which is consistent with the results shown in the theoretical calculations of Figure 5, and the experimental results of Figure 8.

C-scans were also performed on a FRP/Concrete sample in which a delamination was introduced in the FRP “wrap”. Additionally, this sample presented a crack in the concrete running directly underneath the delamination. Figure 10 shows a C-scan image of this sample.

The delamination is visible as the encircled area of light green tones with some red and yellow spots. The crack is visible as a straight strip of light green running upward diagonally from the delamination indication. The undamaged background of the C-scan image is dark green as in the case of the sample with debonded area.

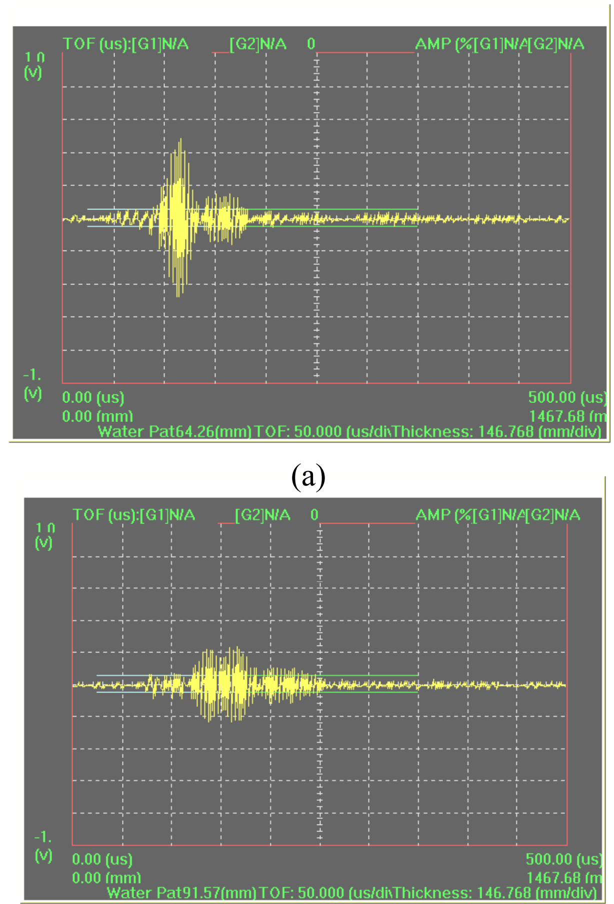

(a)

(b)

Figure 8. RF signals recorded with rolling sensors on an FRP/Concrete sample. (a) Bonded area, (b) Debonded area.

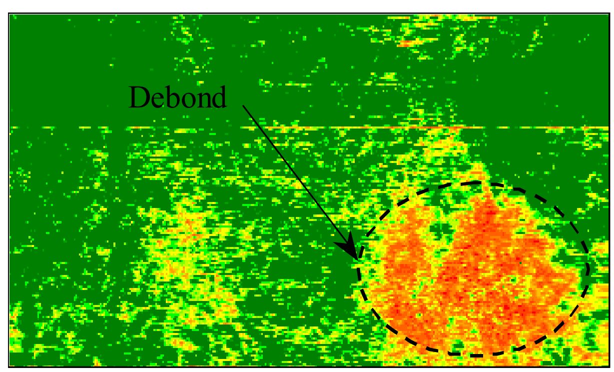

Figure 9. C-scan image of an FRP/Concrete sample showing a debond between the FRP and concrete.

The RF signals shown in Figure 8 and the C-scan images shown in Figures 9 and 10 demonstrated that the Acousto-Ultrasonic technique was a tool that could be used in the inspection of FRP-reinforced concrete structures. Moreover, using the rolling sensors eliminates

the need for an additional coupling medium between the sensor and the structure.

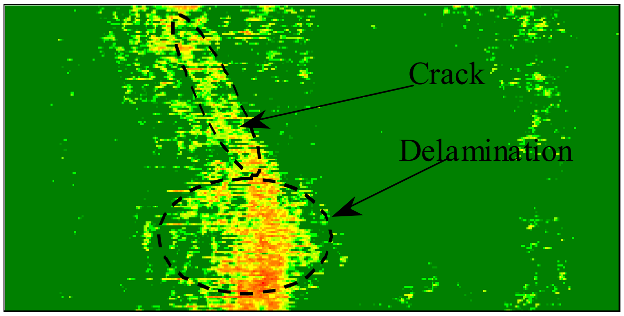

Figure 10. C-scan image of a FRP/Concrete sample showing a delamination inside the FRP and a crack in the concrete below the FRP wrap.

3. PHASE II RESEARCH

The Phase II SBIR started in January 2002 and was completed in January 2004. During this phase of the project PAC designed and constructed FRPCIS, a field-portable, battery-powered, inspection system, for the nondestructive inspection of FRP retrofitted concrete structures. Field trials of the system were performed at Fort Lewis in Tacoma, WA during August 2003 and at ERDC-CERL during October 2003.

3.1 Prototype System Development

The FRP-Concrete Inspection System (FRPCIS) is designed to be field-portable, battery operated and easy to use in an inspection. The specifications of the FRPCIS are:

- Small and portable, with maximum dimensions of 150mm x 150mm x 50mm.
- Battery operated (maximum continuous operation of 8 hrs with rechargeable battery package).
- Capability to detect defects 6mm in diameter.
- PCMCIA interface for data logging storage.
- Capability of generating A- and C-scans.

The FRPCIS meets all the specifications listed above. The system consists of four main components; a CPU platform, an Acousto-Ultrasonic (AU) board, a unique Rolling Sensor Probe (RSP), and Control Software (CS) that allows the different components to communicate and to generate C-scan images.

The FRPCIS is packaged in a white plastic ABS container. This new container is made of fire retardant plastic and is very light. Also, as can be seen in Figure 11, the package contains an integrated removable battery tray and a PCMCIA card slot that are easily accessible for battery change and flash memory removal on the bottom of the package.

(a) (b)

Figure 11. FRPCIS Prototype (a) ABS plastic package with numerical keyboard, (b) Integrated battery tray and PCMCIA card slot.

When access to the battery tray and the PCMCIA card is not necessary, as is the case during inspection, a cover with a rubber gasket can be snapped on to seal the unit. All the connections for the new sensor probe are located on the top-side of the package. Also shown in Figure 11, the FRPCIS has a numerical keypad. This keypad can be used to enter numerical values into the different fields that are used to set up the A- and C-scans. It also contains the system power button.

3.2 Field Testing of FRPCIS

The FRPCIS underwent two separate tests in the field. The first was designed to evaluate the first prototype of FRPCIS with limited A- and C-scan capabilities. This test was performed at Fort Lewis in Tacoma, WA on August 7th, 2003. This location was selected because there were two aging FRP wrapped concrete water storage tanks located in the residential area of the base.

Figure 12. Concrete water tanks reinforced with FRP at Fort Lewis, WA.

The Fort Lewis tanks, shown in Figure 12, were retrofitted with FRP more than 10 years ago and they now show several defects such as debonds, efflorescence, and paint peeling. Also, these tanks present some FRP layer overlap areas.

A total of eleven, one square foot areas were selected around the circumference of the water tanks. Two of these areas had no apparent damage and were considered to be in good condition. These two areas were selected as the baseline for the inspection performed with the first FRPCIS prototype. Nine additional areas that showed evident signs of defects were also selected for inspection.

The eleven areas selected were inspected and C-scan images of each area where generated. The pulsing signal was a square wave pulse of 10 cycles at a frequency of 250 kHz. The scanning areas were 12” by 12”, the scanning direction was from right to left and the resolution in the scanning direction was 0.125”, which is 8 measurements per inch. The indexing direction was from bottom to top and the scanning lines were recorded every 0.5”, giving an image formed of 25 scanning lines.

The C-scan images were formed by assigning a color to every measurement point along a scanning line. The color assigned to every point depends on the value of the signal amplitude recorded at that particular point. The color scale used changes from red for low amplitudes to green for high amplitudes.

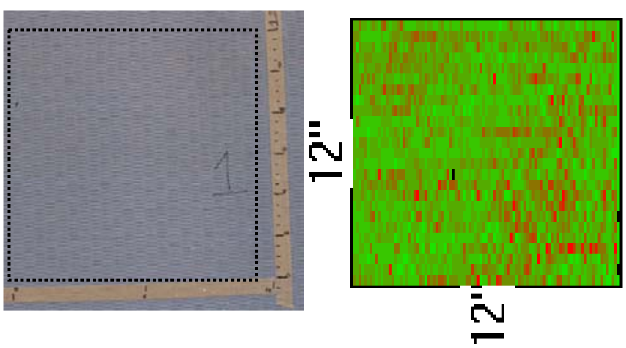

(a) (b)

Figure 13. Water tank area # 1: (a) No defect area, (b) C-scan image covering a 12” by 12” area.

Figure 13(a) shows a picture of the base line area identified as Area 1. In the picture, the dotted square area corresponds approximately to the area that was scanned. This area did not show any visual evidence of damage.

The C-scan image generated in this area, Figure 13(b), shows mostly a green background with some points on red, which indicate an increase in the signal reflected from the FRP. However, these red points do not appear to form a continuous area, which would indicate damage. The red single points most likely were caused by the roughness of the FRP reinforcement surface. When the receiving rolling sensor of the probe hit a rougher than average spot of the FRP surface, the impact could create an acoustic spike that would be detected by the system.

This type of situation could be prevented by selecting the 400 kHz low-pass filters FRPCIS, which was not activated at the time of the inspection.

Figure 14(a) shows a picture of Area 3 that has a debond, separation of the FRP from the concrete, running horizontally along the scanning direction used in generating the C-scan image of Figure 14(b).

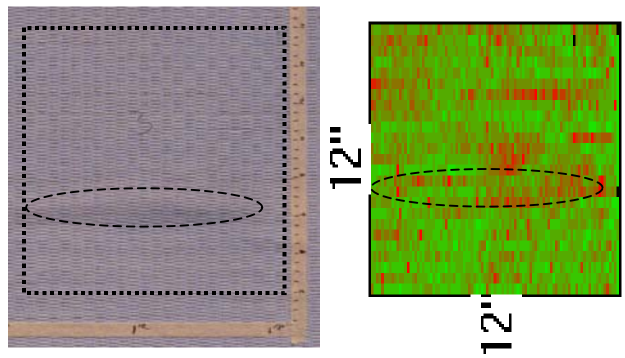

(a) (b)

Figure 14. Water tank area # 3: (a) Area with debond, (b) C-scan image covering a 12” by 12” area.

The dotted oval area indicates the position of the debond. In the C-scan image the approximate area of the debond appears to be delimited by the points in red, although one would expect that the whole area of the debond would appear red. It is possible that the center of the debond did not appear red because lack of good coupling between the rolling sensors and the FRP, since the deformation of the FRP surface was quite large. In order to verify that FRPCIS was indeed detecting the difference between an area with a debond and a good area, RF signals, A-scans, were recorded.

Figure 15 shows a comparison of two A-scans recorded in a section with good bonding and in the center of the debond. The difference between them is clear: the signal recorded in the center of the debond, Figure 15(b), shows a much larger amplitude than the signal recorded in the good bonded part, Figure 15(a). In order to correctly capture this clear difference, an adjustable data recording gate was later designed and added to the FRPCIS software.

The signal corresponding to the debond was obtained by applying pressure to the probe when in position at the center of the dotted oval shown in Figure 14(a) in order to couple it to the deformed FRP surface.

Applying the same type of pressure to the probe while rolling on top of a deformed surface would be difficult, resulting in a lack of coupling between the sensor and the FRP.

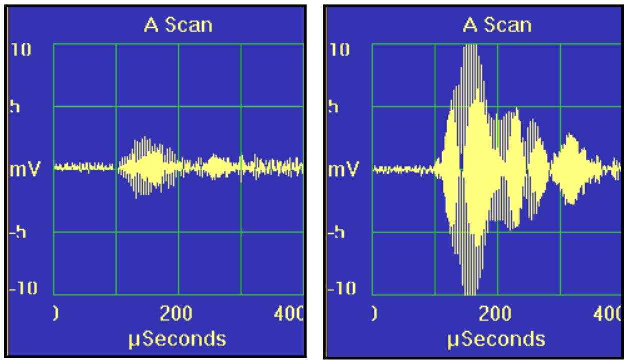

(a) (b)

Figure 15 A-scans recorded on area # 3: (a) Good area, (b) Top of the debonded area.

To improve the coupling when this type of situation arises it was decided that stronger springs would be installed on the probe rolling sensors. The springs installed in FRPCIS provide a constant contact pressure of 20lbs.

One of the aspects that was investigated during this field trial was the effect of overlapping layers of FRP. Figure 16(a) shows Area 6 of the water tank, which had an FRP "patch" on top of the original FRP application. The corresponding C-scan, shown in Figure 16(b), presents no major indications of debonds between the FRP patch and the original application.

The C-scan shows an area of higher reflected signals directly above the FRP patch, indicated by the dotted circle in Figure 16(b). Since there was no visible indication of damaged FRP, as seen in Figure 16(a), this spot could be an indication of small debonds above the FRP patch.

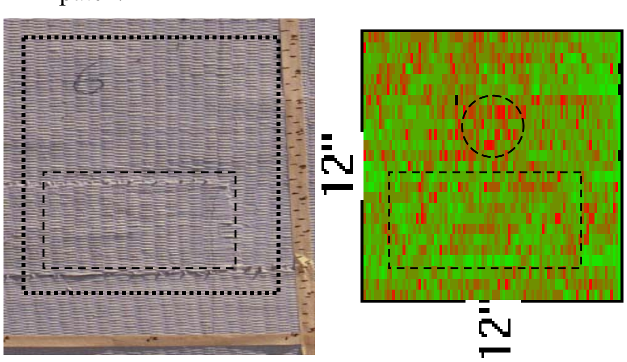

(a) (b)

Figure 16. Water tank area # 6: (a) Area with FRP overlay, (b) C-scan image covering a 12" by 12" area

It is very important to mention that the FRP reinforcement applied to the Fort Lewis water tanks, was very different from the type of reinforcement, which had been used to developed and test FRPCIS during Phase I and Phase I Option. However, the system was able to detect some of the differences between undamaged and damaged areas.

3.3 Test at CERL in Champaign, IL.

After the data obtained during the first test were analyzed, the results were used to improve the A- and C-scan capabilities of the FRPCIS software. The improved software was then tested in a second FRPCIS prototype. This second field trial of FRPCIS was conducted at CERL on October 7th, 2003. The test was conducted on a scale model of a fire station that was built and tested at CERL. The half-scale model was subjected to simulated seismic loads and reinforced with FRP in critical points of the structure, before being subjected to simulated seismic loads.

Four different types of FRP reinforcement were installed in the interior of the model's ground floor. These different types of reinforcements were installed so CERL could investigate their performance under severe loads. The test focussed on the glass/epoxy type of FRP, similar to that used in the Concrete-FRP samples that were prepared by PAC. The FRP reinforcement was installed inside the half-scale model. The reinforcement was installed in strips approximately three inches wide.

Five different areas reinforced with glass FRP were selected for inspection. Four of these had written indications to denote the presence of debonds and one did not present any visual indication of damage. Some areas included vertical FRP strips, others had an FRP strip oriented at 45 degrees and overlaps between vertical and angled strips.

One area inspected in the half-scale model of the firehouse included an FRP strip, which was oriented at 45 degrees from the vertical direction as shown in Figure 17. This FRP section was marked as containing two damaged areas. C-scan images of these two areas were generated, one was 1" by 3" and another 1" by 6".

Both C-scan images are shown in Figure 17. The shorter of the two scans shows the damaged area located close to the edge of the FRP, while the larger of the scans shows the damage on the vertical direction across the FRP strip. The location and orientation of the damaged areas in the C-scan images correspond to the locations and orientation indicated in the FRP strips.

One problem that was encountered during the field test of FRPCIS was the width of the reinforcement area. Since the firehouse model was half-scale, the FRP

reinforcement was also half-scale. This rendered the inspection area too narrow to accommodate wide scans. Another problem encountered was the application of the FRP reinforcement. The edges of the FRP strips contained splintered glass fibers. These fibers were pointed upwards most of the time and hit the RSP metal skirt. This factor limited the scanning area even more. The combination of these two factors limited the scanning area width to 1". In order to avoid these types of problems in future inspections it was decided to shorten the metal skirt of the RSP. This modification has been introduced in the final version of the FRPCIS.

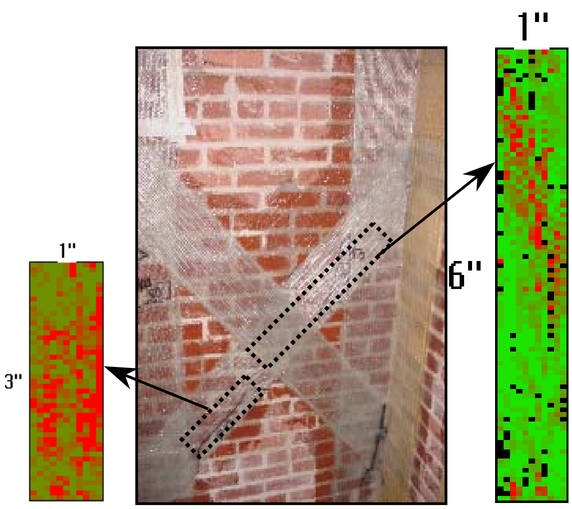

Figure 17. Area of glass-FRP reinforcement with two (2) indications of damage.

4.0 CONCLUSIONS

A Nondestructive Evaluation Technique for the inspection of FRP reinforced civil structures was successfully developed during Phase I and Phase I Option of the SBIR program. Also, a portable FRP-Concrete Inspection System (FRPCIS) was designed, constructed and tested during Phase II.

FRPCIS is capable of detecting defects in FRP reinforced structures. FRPCIS can detect debonds of 0.25 inch in diameter. The system is capable of generating A- and C-scan images of defects. Based on the theoretical model the inspection frequency can be optimized for the detection and imaging of defects in a particular type of composite

FRPCIS was demonstrated on FRP reinforced concrete water tanks at Fort Lewis, WA in August 2003, and in a half-scale mockup of a firehouse in October 2003, at CERL. Also extensive testing and demonstration was conducted on FRP-retrofitted concrete samples with seeded defects at PAC. The final FRPCIS prototype was demonstrated and delivered to ERDC-CERL on January 12th, 2004.

Several observations were made during the course of the Phase II effort where system enhancements or modified inspection techniques could lead to improved performance of the FRPCIS.

One immediate modification that will have an important impact on the applications of the FRPCIS is the introduction of angle beam rolling sensors. Such a modification will increase the penetration of the acoustic signals. With increased penetration, the system could be used to inspect thick-multilayered composites such as those used in composite armor (Godinez et al, 2001).

The inclusion of USB capabilities in the FRPCIS would make it very versatile. The dependence on a particular type of PDA would be eliminated, and connectivity to Laptop and other pocket computers will be possible.

REFERENCES

Godínez, V. F., Finlayson, R. D., and Miller, R. K., 2002: Acousto-Ultrasonics: A tool for Nondestructive Evaluation of Multi-layer Composites, *Proceedings of the American Society for Composites 17th Technical Conference*, October 21-23, 2002. West Lafayette, IN.

Godínez, V. F., Finlayson, R. D., and Miller, R. K., and Raju, B. B., 2001: Acousto-Ultrasonic Inspection of Hybrid Composite Armor Plate, *Review Progress in Quantitative Nondestructive Evaluation,* Vol. 20, American Institute of Physics, New York.

Godínez, V. F., Carlos, M. F., Delamere, M., Hoch, W., Fotopoulos, C., and Raju, B. B., 2001: Acousto-Ultrasonic System for the Inspection of Composite Armored Vehicles, *Review Progress in Quantitative Nondestructive Evaluation,* Vol. 20, American Institute of Physics, New York.

Ji, Y., Sullivan, R. and Balasubramanian, K., 1995: Guided Wave Behavior Analysis in Multi-Layered Inhomogeneous Anisotropic Plates, *Proceedings of the Twenty-Second Review Progress in QNDE*, Seattle Washington, July 30-August 4, 1995, Vol 15, Thompson, D.O. and Chimenty, D.E., Eds, (Plenum, New York, 1996), pp. 217-222.